ISSN 0023-1584, Kinetics and Catalysis, 2006, Vol. 47, No. 2, pp. 234–240. © MAIK "Nauka/Interperiodica" (Russia), 2006.

Theoretical Investigation of Novel Silsesquioxane-Supported Phillips-Type Catalyst by Density Functional Theory (DFT) Method[1]

B. Liu, Y. Fang, W. Xia, and M. Terano

School of Materials Science, Japan Advanced Institute of Science and Technology, 1-1 Asahidai, Tatsunokuchi, Ishikawa 923-1292, Japan
e-mail: boping@jaist.ac.jp

Received July 11, 2005

Abstract—In spite of great commercial importance of the Phillips CrO_x/SiO_2 catalyst and long term research efforts, the precise physicochemical nature of active sites and polymerization mechanisms still remains unclear. The difficulties in a clear mechanistic understanding of this catalyst mainly come from the complexity of the surface chemistry of the amorphous silica gel support. In this work, novel silsesquioxane-supported Phillips Cr catalysts are utilized as realistic models of the industrial catalyst for theoretical investigation using the density functional theory (DFT) method in order to elucidate the effects of surface chemistry of silica gel in terms of supporting of chromium compounds and fluorination of the silica surface on the catalytic properties of the Phillips catalyst. Both qualitative and quantitative aspects with respect to various electronic properties and thermodynamic characteristics of the model catalysts were achieved. The future prospects of a state-of-the-art catalyst design and mechanistic approaches for the heterogeneous SiO_2-supported Phillips catalyst has been demonstrated.

DOI: 10.1134/S0023158406020121

INTRODUCTION

As one of the most important industrial olefin polymerization catalysts, the Phillips catalyst is still producing several million tons of high-density polyethylene (HDPE) featuring ultrabroad molecular weight distribution and long chain branching [1]. These unique polymer structures give rise to ideal polymer properties for both processing, especially, blow molding and final applications [1, 2]. Compared with the preparation process of other kinds of olefin polymerization catalysts, calcined Phillips $Cr(VI)O_x/SiO_2$ catalyst can be easily synthesized through a calcination procedure after impregnation of a chromium compound (chromium trioxide or chromium acid, etc.) on porous amorphous silica gel. Those chromium compounds could be supported on the silica gel surface through chemical reactions with surface hydroxyl groups on silica gel [2]. The calcined Phillips $Cr(VI)O_x/SiO_2$ catalyst must be further activated through reduction into $Cr(II)O_x/SiO_2$ either by ethylene monomer (C_2H_4), carbon monoxide (CO), or Al-alkyl cocatalysts (e.g., triethylaluminum (TEA)) for ethylene polymerization [2]. As a matter of fact, the real physicochemical nature of active sites and polymerization mechanisms are still open for discussion even after 50 years of great efforts since its discovery in the early 1950s [3]. Owing to its commercial importance as well as poor mechanistic understanding, today the Phillips catalyst is still attracting great academic interest from both experimentalists [4–14] and theoreticians [15, 16].

The key to achieving a solution to these long-standing questions is to obtain specific information about the precise chemical structures and electronic properties of surface chromium species as active precursors on a Phillips-type catalyst [2, 3]. In fact, the great difficulties in mechanistic studies on Phillips catalyst lie in the heterogeneity of the catalytic species on the amorphous silica gel surface. It is well known that the catalytic properties of the Phillips catalyst depend drastically on the calcination conditions as well as surface modification of the silica gel support [2, 3]. For example, fluorination of the silica gel surface could significantly improve the catalytic performance according to previous reports [2, 17]. However, precise identification of those surface chromium species as active precursors in terms of precise chemical structures and electronic properties after surface ligand modification on silica gel is very difficult solely based on experimental approaches. Recently, some theoretical approaches based on chromium species supported on various small siloxane cluster models were reported to be efficient in achieving a deeper understanding of the polymerization mechanisms of a Phillips-type catalyst [15, 16]. More recently, we reported the molecular orbital origin of the driving force for the intermolecular orientation-directed reaction between ethylene monomer and a

[1] The text was submitted by the authors in English.

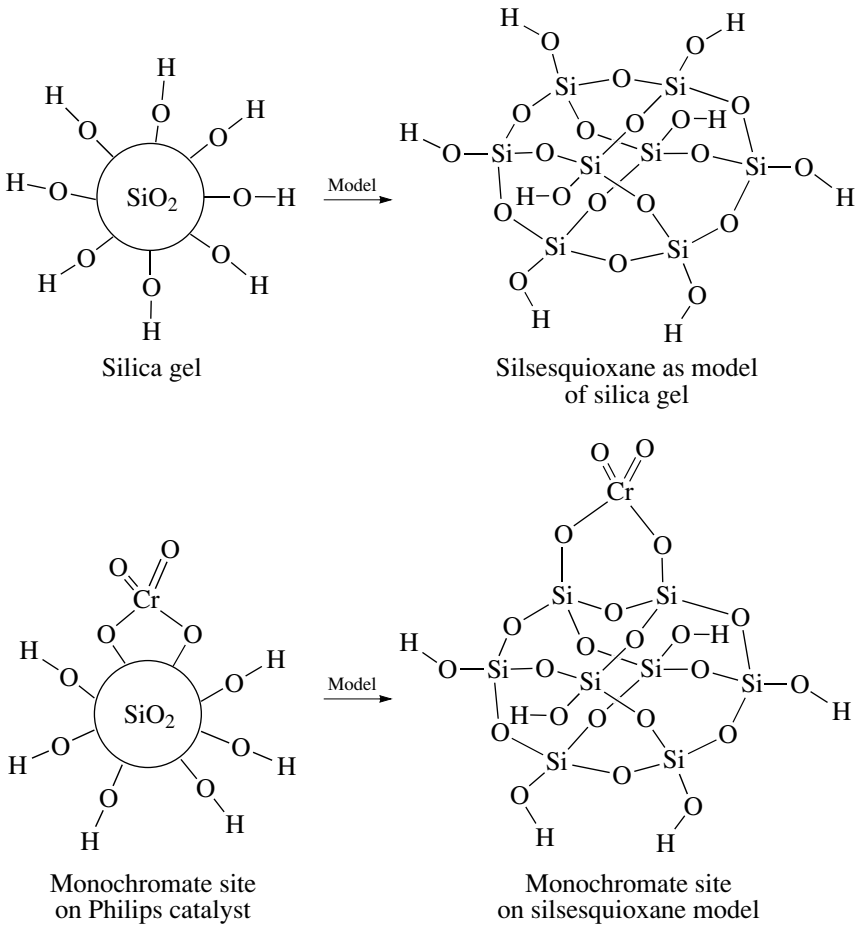

Fig. 1. Silica gel versus silsesquioxane model and monochromate sites on Phillips CrO_x/SiO_2 catalyst versus monochromate sites on silsesquioxane model.

monochromate Cr(VI) site utilizing chromic acid as a simple cluster model [18]. However, all those abovementioned small cluster models are difficult to use for further theoretical investigation on the significant effects from the surface chemistry of silica gel support on the catalytic behaviors of Phillips-type catalyst. It is necessary to consider a more realistic model for silica gel support.

In recent years, silsesquioxane has been proven to be an ideal model of silica gel [19]. Moreover, various transition metal catalysts supported on silsesquioxane have been experimentally proven to be realistic model catalysts for olefin polymerization [20]. In this work, a fully hydroxylated silsesquioxane was used as the model of silica gel for synthesizing a silsesquioxane-supported Phillips-type catalyst (Fig. 1). As a preliminary approach, the equilibrium geometry and electronic properties of monochromate Cr(VI) sites and divalent Cr(II) sites were investigated in terms of ligand variation from hydroxyl (–OH) to fluorine (–F) on silsesquioxane. The calculated results shown in this work have qualitatively and quantitatively demonstrated that fluorination of the silica gel surface could create significant effects on the electronic nature of the active Cr precursors on Phillips catalysts.

COMPUTATIONAL METHOD

The equilibrium structures of molecular models (Model Sites **1**–**4** as shown in Fig. 2) of monochromate Cr(VI) sites and divalent Cr(II) sites supported on silsesquioxane in the ground state in terms of ligand variation from hydroxyl to fluorine were calculated by the DFT method (RB3LYP, basis set 6-31G**, multiplicity: singlet for Cr(VI) sites and triplet for Cr(II) sites) using SPARTAN'02 Windows developed by Wavefunction, Inc. [21]. The surface electron density, surface potential, the highest occupied molecular orbital (HOMO), the lowest unoccupied molecular orbital (LUMO), dipole moment, and electrostatic charges of each site were obtained. The thermodynamic characteristics of the supporting reaction of chromium compounds (chromium trioxide or chromium acid) on silsesquioxane and subsequent activation reactions of chromate species by ethylene monomer, carbon monoxide, and triethylaluminum before ethylene polymer-

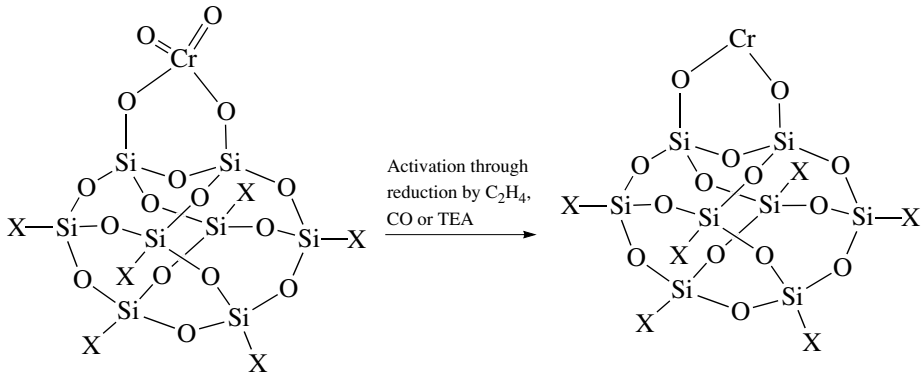

1 (X = –OH)
2 (X = –F)

3 (X = –OH)
4 (X = –F)

Fig. 2. Model sites (**1**–**4**) in terms of ligand variation from hydroxyl to fluorine on the monochromate Cr(VI) sites and divalent Cr(II) sites supported on silsesquioxane. Ligand X = –OH or –F.

ization were investigated on the basis of the energy level of each species at the ground state.

RESULTS AND DISCUSSION

The optimized equilibrium geometry structures of model sites **1** and **2** were calculated using the DFT RB3LYP method with a 6-31G** basis set. The equilibrium structure parameters of model sites **1** and **2** are shown in Table 1, including a comparison with the equilibrium structure of chromic acid [18]. Model site **1** corresponds to the process of supporting chromic acid on silsesquioxane, while model site **2** is indicative of the process of further fluorination of the silsesquioxane surface. As can be seen from Table 1, the bond length of Cr=O is shortened from 1.562 to 1.558 Å after the chromic acid was supported on the silsesquioxane. The Cr=O bond was further shortened to 1.555 Å after fluorination of the fully hydroxylated silsesquioxane. Accordingly, the bond length of Cr–O was elongated from 1.754 to 1.762 and 1.768 Å from chromic acid to model site **1** and model site **2**. Both the bond angles of O=Cr=O and O=Cr–O were enlarged due to supporting of the chromic acid on silsesquioxane and subsequent fluorination of hydroxyl groups, and accordingly the bond angles of O–Cr–O were going in the opposite direction.

The optimized equilibrium geometry, the highest occupied molecular orbital, the lowest unoccupied molecular orbital, electron density, and electrostatic potential of the hexavalent monochromate sites **1** and **2** are shown in Fig. 3. As shown in Fig. 3, the LUMO of model sites **1** and **2** consisted mostly of atomic orbitals from the atoms around the Cr center. The HOMO of model sites **1** is mainly contributed from atoms far away from the Cr center, while the HOMO of model sites **2** is derived from atomic orbitals from all over the whole molecule. Regarding the electrostatic potential of model sites **1** and **2**, shown in Figs. 3d and 3h, the negative electrostatic charges were more concentrated on oxygen atoms for model **1**, while they were more homogeneously distributed on model **2** most probably due to the electron-abstracting effect of the fluorine ligand.

The optimized equilibrium geometry structures of model sites **3** and **4** were calculated using the DFT

Table 1. Equilibrium geometry of hexavalent monochromate Cr(VI) model sites supported on silsesquioxane calculated by the DFT method and a comparison with chromic acid

Geometry parameters of Cr(VI) models and chromic acid*		Chromic acid*	Model site **1** ligand X = –OH	Model site **2** ligand X = –F
Bond lengths, Å	Cr=O	1.562	1.558	1.555
	Cr–O	1.754	1.762	1.768
Bond angles, deg	O=Cr=O	107.83	108.85	108.89
	O=Cr–O	109.60	110.49	110.59
	O–Cr–O	110.57	106.02	105.58

Note: Computation conditions: DFT method RB3LYP, basis set: 6-31G**, multiplicity: singlet.

* Data from our previous report [18].

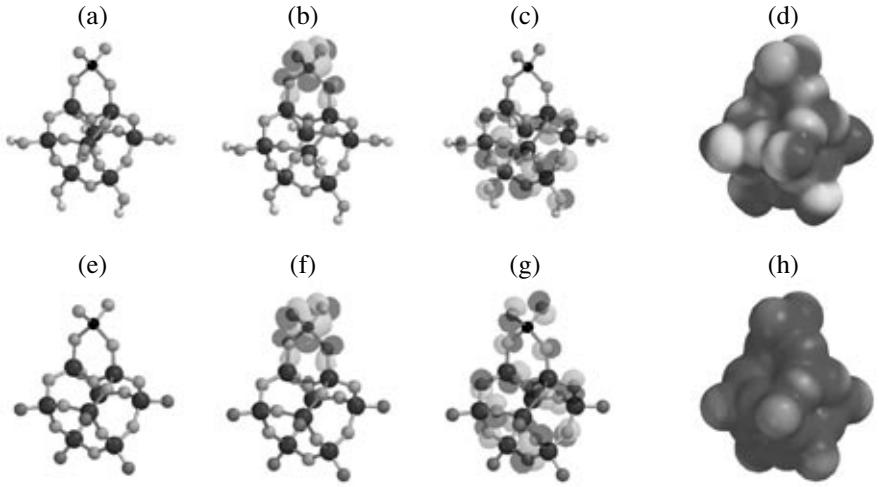

Fig. 3. Equilibrium geometry (a, e), the elements are coded in an increasing gray scale sequence as follows: H (white) < O < F < Si < Cr (black)); LUMO (b, f), black and gray clouds indicate positive and negative phase, respectively); HOMO (c, g), black and gray clouds indicate positive and negative phase, respectively); electron density and electrostatic potential (d, h), dark indicates positive charge, and light indicates negative charge) of hexavalent monochromate Cr(VI) sites supported on silsesquioxane computed by the DFT method; for (a–d), ligand X = –OH (model site **1**); for (e–h), ligand X = –F (model site **2**).

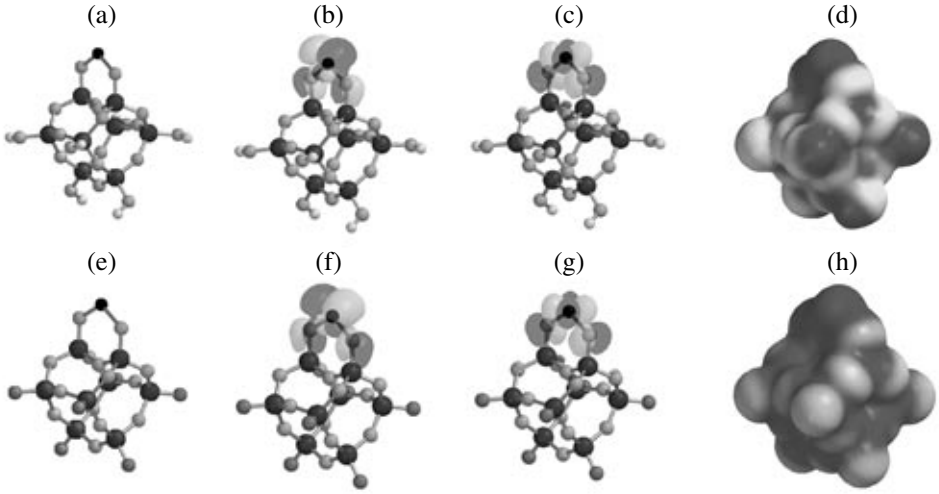

Fig. 4. Equilibrium geometry (a, e), the elements are coded in an increasing gray scale sequence as follows: H (white) < O < F < Si < Cr (black)); LUMO (b, f), black and gray clouds indicate positive and negative phase, respectively); HOMO (c, g), black and gray clouds indicate positive and negative phase, respectively); electron density and electrostatic potential (d, h), dark indicates positive charge, and light indicates negative charge) of divalent Cr(II) sites supported on silsesquioxane computed by the DFT method; for (a–d), ligand X = –OH (model site **3**); for (e–h), ligand X = –F (model site **4**).

RB3LYP method with a 6-31G** basis set. The equilibrium structure parameters of model sites **3** and **4** are shown in Table 2. Model sites **3** and **4** correspond to the divalent active site precursors after activation of **1** and **2** through reduction by ethylene, CO, or TEA in terms of ligand variation from hydroxyl to fluorine. As can be seen from Table 2, bond lengths of Cr–O were elongated for both model site **3** and model site **4** after reduction from model site **1** and model site **2**, respectively. Accordingly, the bond angle of O–Cr–O was significantly increased owing to the reduction of **1** and **2**.

The optimized equilibrium geometry, HOMO, LUMO, electron density, and electrostatic potential of the divalent sites **3** and **4** are shown in Fig. 4. As shown in Fig. 4, both the LUMO and HOMO of model sites **3** and **4** consist mostly of atomic orbitals from the atoms around the Cr center. Regarding the electrostatic potential of model sites **3** and **4**, shown in Figs. 4d and 4h, the negative electrostatic charges were more concentrated on oxygen atoms for model **3**, while they were more homogeneously distributed on model **4** most probably also due to the electron-abstracting effect of the fluorine ligand.

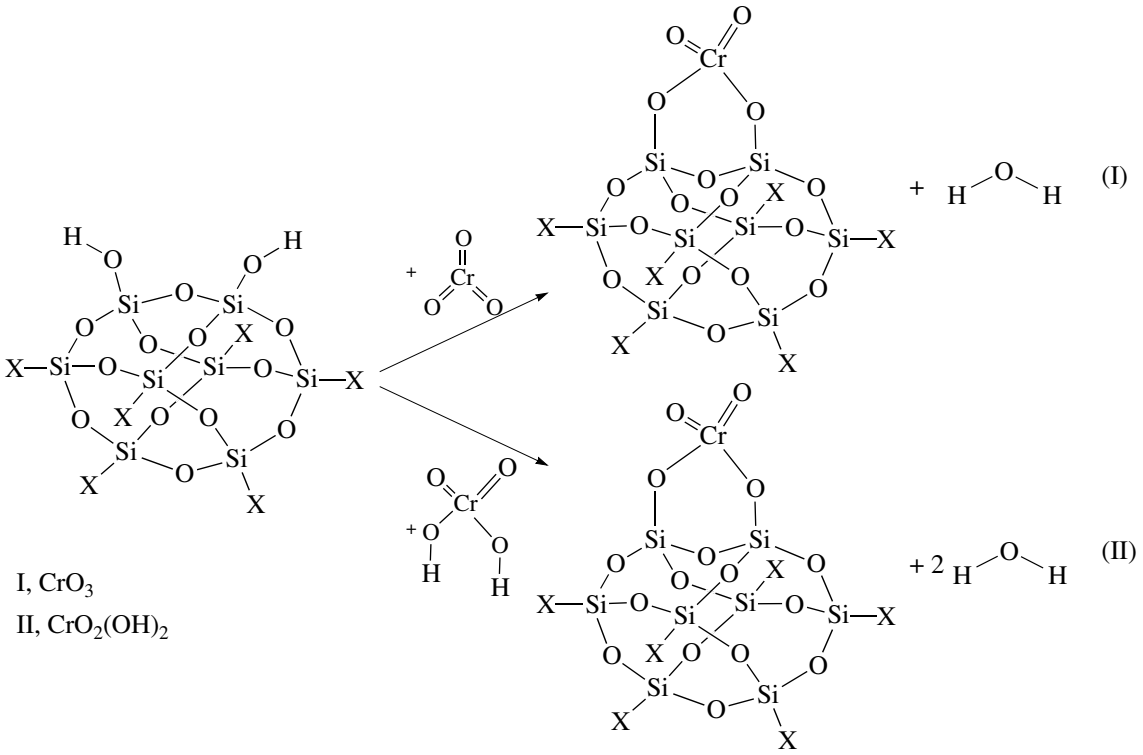

Scheme 1. Supporting reactions of chromium compounds on silsesquioxane (ligand X = –OH or –F).

The energy of HOMO (E_{HOMO}), energy of LUMO(E_{LUMO}), band gap (BG), dipole moments (DM), and electrostatic charges of chromium (ESCC) for the Cr(VI) and Cr(II) model sites (**1**–**4**) at equilibrium geometry are shown in Table 3 with a comparison with chromium acid. The supporting effect of the chromic acid on silsesquioxane and the ligand effect of the silsesquioxane on the electronic properties of the model sites (**1**–**4**) could be clearly observed. As can be seen, both supporting of the chromic acid on silsesquioxane and further fluorination of the silsesquioxane surface decrease the energies of LUMO and HOMO as well as

Table 2. Equilibrium geometry of divalent Cr(II) model sites supported on silsesquioxane calculated by the DFT method

Geometry parameters of Cr(II) models	Model site **3** ligand X = –OH	Model site **4** ligand X = –F
Cr–O bond lengths, Å	1.843	1.849
O–Cr–O bond angles, deg	118.92	116.83

Note: Computation conditions: DFT method RB3LYP, basis set: 6-31G**, multiplicity: triplet.

Table 3. Energy of HOMO (E_{HOMO}), energy of LUMO (E_{LUMO}), band gap (BG), dipole moments (DM), and electrostatic charges of chromium (ESCC) for the Cr(VI) and Cr(II) model sites supported on silsesquioxane at equilibrium geometry and a comparison with chromium acid calculated by DFT method

Model sites	Ligand X	Cr oxidation state	E_{HOMO}, eV	E_{LUMO}, eV	BG, eV	DM, Debye	ESCC
Cr Acid*	–	+6	–8.66	–4.52	4.14	4.48	+0.887
1	–OH	+6	–8.79	–4.86	3.93	4.40	+0.813
2	–F	+6	–9.74	–5.55	4.19	0.62	+0.797
3	–OH	+2	–6.72	–2.94	3.78	4.39	+1.019
4	–F	+2	–7.39	–3.54	3.85	8.46	+1.085

Note: Computation conditions: DFT method RB3LYP, basis set: 6-31G**, multiplicity: singlet for Cr(VI) and triplet for Cr(II).

* Data from our previous report [18].

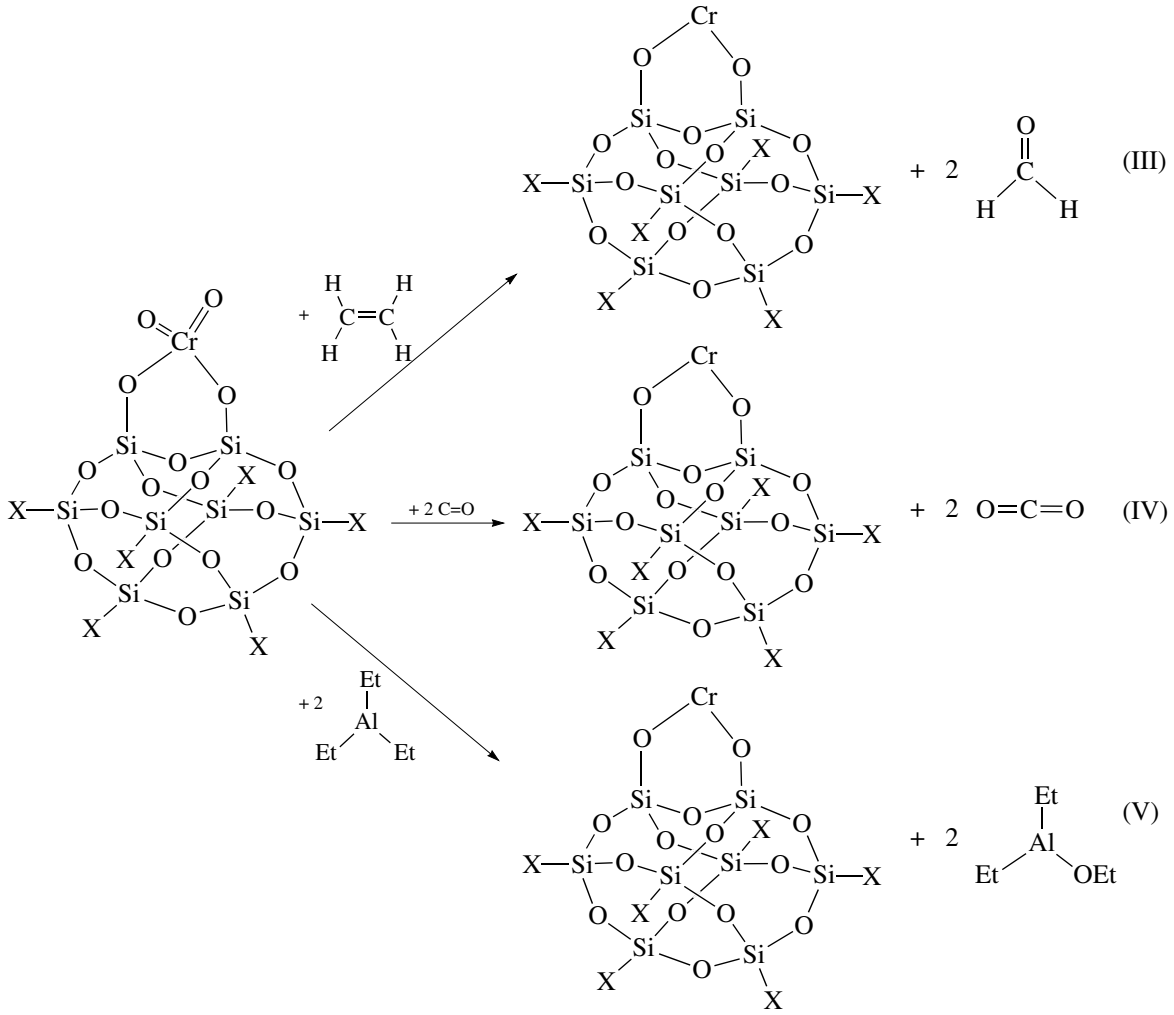

Scheme 2. Activation reactions through reduction of monochromate Cr(VI) sites into Cr(II) sites supported on silsesquioxane (ligand X = –OH or –F) by ethylene monomer (III); carbon monoxide (IV); triethylaluminum (TEA) cocatalyst (V).

the positive charges on sites **1** and **2**. In general, the reduction of sites **1** and **2** into sites **3** and **4** significantly increases the energies of LUMO, HOMO, and positive charges of the Cr centers, while it decreases the band gap simultaneously. This evidence indicates that sites **3** and **4** should be chemically much more active than sites **1** and **2**, which is consistent with the experimental fact that sites **3** and **4** must be reduced into sites **1** and **2** for ethylene polymerization.

The thermodynamic characteristics of the supporting reactions (shown in Scheme 1 [2, 6, 7]) of chromium compounds (chromium trioxide or chromium

Table 4. Heat of reactions (ΔH, kJ/mol) for supporting of chromium compounds (chromium trioxide or chromium acid) on silsesquioxane and subsequent activation of the hexavalent monochromate Cr(VI) species into divalent Cr(II) precursors by ethylene monomer (C_2H_4), carbon monoxide (CO) or triethylaluminum (TEA) for the silsesquioxane-supported Phillips type catalyst calculated by the DFT method

Reactions*	(I)	(II)	(III)	(IV)	(V)
Ligand X	ΔH_1	ΔH_2	ΔH_3	ΔH_4	ΔH_5
–OH	–182.7	+22.3	+105.5	–236.3	–254.6
–F	–169.6	+35.4	+89.5	–252.3	–270.6

Note: Computation conditions: DFT method RB3LYP, basis set: 6-31G**, multiplicity: singlet for Cr(VI) and triplet for Cr(II).

* Corresponding to reaction numbers shown in Schemes 1 and 2.

acid) on silsesquioxane and subsequent activation reactions (shown in Scheme 2 [11, 12]) of chromate species by ethylene monomer, carbon monoxide, and triethylaluminum before ethylene polymerization were investigated on the basis of the energy level of each species at the ground state. The heats of reactions (ΔH) for the supporting (reactions (I) and (II) shown in Scheme 1) and subsequent activation (reactions (III), (IV) and (V) shown in Scheme 2) are tabulated in Table 4. The results show that CrO_3 is much more thermodynamically favorable to be supported on silsesquioxane than chromic acid. Fluorination of silsesquioxane does not thermodynamically favor the supporting process for either CrO_3 or chromic acid. It is also found that TEA cocatalyst and CO both are most thermodynamically favorable to activate the hexavalent sites **1** and **2** into divalent active precursors **3** and **4** for ethylene polymerization, while ethylene monomer is not a good activator thermodynamically, which are consistent with the experimental fact that there is usually an induction period when using ethylene monomer as activator, while the induction period disappears when TEA or CO are used as activator for ethylene polymerization with Phillips-type catalysts [2]. It is also very interesting to demonstrate that fluorination of silsesquioxane surface is quite thermodynamically favorable to the activation reactions for ethylene polymerization using either ethylene, CO, or TEA. This computational evidence also strongly supports the promotional effect from fluorination of the surface of Phillips catalysts for ethylene polymerization [2, 17].

CONCLUSIONS

In this work, novel silsesquioxane-supported Phillips Cr catalysts are utilized as realistic models of the industrial catalyst for theoretical investigation using the density functional theory (DFT) method in order to develop a methodology for theoretical study of the effects of surface chemistry of silica gel in terms of ligand variation on the catalytic properties of the Phillips catalyst. It has been demonstrated that a theoretical understanding of the supporting effect of chromium compounds and fluorination of the silica surface on the physicochemical nature of active Cr precursors as well as their catalytic performance (e.g., activation reaction) of the Phillips catalyst has been obtained through DFT calculations. Both qualitative and quantitative aspects with respect to various electronic properties and thermodynamic characteristics of the model catalysts have been achieved. The future prospects for a state-of-the-art catalyst design and mechanistic approaches for the heterogeneous SiO_2-supported Phillips catalyst has been demonstrated in this preliminary approach. Further theoretical investigations are still in progress in order to elucidate the polymerization mechanisms of the Phillips catalyst in terms of surface ligand modification.

REFERENCES

1. Pullukat, T.J. and Hoff, R.E., *Catal. Rev.—Sci. Eng.*, 1999, vol. 41, p. 389.
2. McDaniel, M., *Adv. Catal.*, 1985, vol. 33, p. 47.
3. Groppo, E., Lamberti, C., Bordiga, S., Spoto, G., and Zecchina, A., *Chem. Rev.*, 2005, vol. 105, p. 115.
4. Gaspar, A.B., Brito, F.J.L., and Dieguez, L.C., *J. Mol. Catal. A: Chem.*, 2003, vol. 203, p. 251.
5. Bordiga, S., Bertarione, S., Damin, A., Prestipino, C., Spoto, G., Lamberti, C., and Zecchina, A., *J. Mol. Catal. A: Chem.*, 2003, vols. 204–205, p. 527.
6. Liu, B. and Terano, M., *J. Mol. Catal. A: Chem.*, 2001, vol. 172, p. 227.
7. Liu, B., Fang, Y., and Terano, M., *J. Mol. Catal. A: Chem.*, 2004, vol. 219, p. 165.
8. Fang, Y., Liu, B., and Terano, M., *Appl. Catal., A*, 2005, vol. 279, p. 131.
9. Liu, B., Nakatani, H., and Terano, M., *J. Mol. Catal. A: Chem.*, 2002, vol. 184, p. 387.
10. Liu, B., Nakatani, H., and Terano, M., *J. Mol. Catal. A: Chem.*, 2003, vol. 201, p. 189.
11. Liu, B., Fang, Y., Nakatani, H., and Terano, M., *Macromol. Symp.*, 2004, vol. 213, p. 37.
12. Fang, Y., Liu, B., Hasebe, K., and Terano, M., *J. Polym. Sci., Part A: Polym. Chem.*, 2005, vol. 43, p. 4632.
13. Liu, B., Šindelář, P., Fang, Y., Hasebe, K., and Terano, M., *J. Mol. Catal. A: Chem.*, 2005, vol. 238, p. 142.
14. Fang, Y., Liu, B., and Terano, M., *Kinet. Katal.*, 2006, vol. 47, p. 297 [*Kinet. Catal.* (Engl. Transl.), 2006, vol. 47, no. 2, p. 295].
15. Schmid, R. and Ziegler, T., *Can. J. Chem.*, 2000, vol. 78, p. 265.
16. Espelid, O. and Borve, K.J., *J. Catal.*, 2002, vol. 205, p. 366.
17. Rebenstorf, B., *J. Mol. Catal.*, 1991, vol. 66, p. 59.
18. Liu, B., Fang, Y., and Terano, M., *Mol. Simul.*, 2004, vol. 30, p. 963.
19. Dijkstra, T.W., Duchateau, R., van Santen, R.A., Meetsma, A., and Yap, G.P.A., *J. Am. Chem. Soc.*, 2002, vol. 124, no. 33, p. 9856.
20. Duchateau, R., *Chem. Rev.*, 2002, vol. 102, no. 10, p. 3525.